Joint SIG Workshop

Urban - 3D - Radar - Thermal Remote Sensing and Developing Countries

Ghent, 22-24 September 2010

Book of Proceedings

EUROPEAN ASSOCIATION OF REMOTE SENSING LABORATORIES

Sponsored by

Ghent University, Het Pand,
Onderbergen 1, 9000 Ghent (Belgium

Use of multi-angle high-resolution imagery and 3D information for urban land-cover classification: a case study on Istanbul

Marc Binard [1], Frederik Tack [2] , Tim Van de Voorde [3], Yves Cornet [4] and Frank Canters [5]

1. Université de Liège, SURFACES, Geomatics Unit, Liège, Belgium; marc.binard@ulg.ac.be
2. Universiteit Gent, Department of Geography, Gent, Belgium; f.tack@ugent.be
3. Vrije Universiteit Brussel, Department of Geography, Brussels, Belgium; tvdvoord@vub.ac.be
4. Université de Liège, SURFACES, Geomatics Unit, Liège, Belgium; ycornet@ulg.ac.be
5. Vrije Universiteit Brussel, Department of Geography, Brussels, Belgium; fcanters@vub.ac.be

ABSTRACT

The BELSPO-MAMUD project focuses on the use of remote sensing data for measuring and modelling urban dynamics. Remote sensing is a wonderful tool to produce long time-series of sealed surface maps, which are useful for this purpose. In the urban context of Istanbul, a very dynamic city, recent high resolution satellite images and medium resolution images from the past have been exploited to calibrate and validate a regression-based sub-pixel classification method allowing this production.

Image classification in an urban context is a tricky task for several reasons: prominent occurrence of shadowed and occluded areas and urban canyons, spectral confusions between urban and non-urban materials at ground and roof levels, moderately hilly relief ... To cope with these difficulties the combined use of three types of data may be helpful: diachronic (vii), multi-angle and 3D data.

A master multispectral and panchromatic QuickBird image and a panchromatic Ikonos stereopair, all acquired in March 2002, were used in combination with a multispectral and panchromatic Ikonos image of May 2005. A DSM was generated from the Ikonos stereopair and building vector file. It was used for orthorectification, building height estimation and classification. The area covered by the high resolution products was divided in 3 parts and each was classified independently.

This application demonstrates that a recent high resolution land-cover classification produced using multi-date, multi-angle and DSM can be used to produce sealed surface maps from longer time-series of medium resolution images over large urban areas, thus enabling the analysis of urban dynamics.

Keywords: remote sensing, classification strategy, sub-pixel classification, DSM, urban dynamics, sealed surface.

INTRODUCTION

All over the world, urbanization is an increasing phenomenon that produces many environmental perturbations. One of the characteristics of this urbanization is the increase of the area covered by sealed surfaces causing runoff increase (vii), urban overheating with implication on health (vii) and pollutant washing associated with non point source or diffuse pollution (vii). In the EU, the increase of sealed surfaces cover is seen as a major problem that must be tackled.

In the framework of the BELSPO-MAMUD project (vii), a research initiative that focuses on the use of remote sensing data for measuring and modelling urban dynamics, the increase of sealed surface area is one of the major parameters taken into consideration. To produce long time series of high resolution sealed surface maps of the very dynamic city of Istanbul we used a sub-pixel classification method of medium resolution (MR) satellite imagery. To calibrate and validate the sub-pixel classification models, an accurate high-resolution (HR) land-cover map was required for a representative part of the city area. Producing a HR land-cover map in this specific urban context is a tricky task for several reasons: prominent occurrence of shadowed and occluded areas and urban canyons, spectral confusion between urban and non-urban materials at ground and roof level, moderately hilly relief ... To cope with these difficulties, we combined three types of data in a HR image classification procedure : (1) diachronic data to reduce shadow from summer images, (2) images with various satellite elevation and azimuth angles to reduce occluded areas, (3) 3D data to discriminate land-covers with similar signature at the ground and roof levels.

METHODS

Study material

A master multispectral and panchromatic QuickBird image acquired during March 2002 is used in combination with a multispectral and panchromatic Ikonos image of May 2005. The influence of solar angle and satellite geometric configuration on both images is clearly illustrated on figure 1. The QuickBird image shows longer shadows than the Ikonos image. Shadow directions are nearly the same because of similar sun-time acquisition. Concerning direction and size of the slant effect producing occlusions, the same figure shows a smaller displacement on the Ikonos image. On the QuickBird image, displacement is nearly in the same direction as the shadows. In the two cases, areas hidden by buildings (occluded area) are clearly smaller than areas affected by shadows.

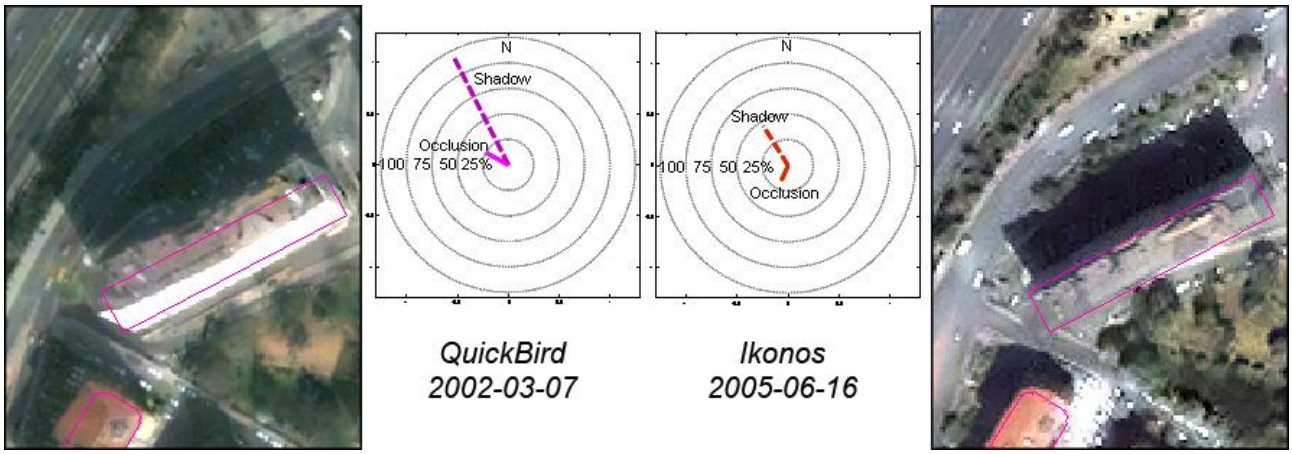

Figure 1: Shadowed and occluded areas are respectively related to sun and satellite positions (shadow and occlusion lengths are given in % of the building height)

A panchromatic Ikonos stereo-pair acquired in March 2002 was also used to form a triplet with the Ikonos image acquired in May 2005 (Figure 2). A DSM was produced using this triplet. It provides the 3D information that is exploited in the classification strategy described here after.

The Istanbul Metropolitan Planning Centre (IMP-Bimtas) provided us a large-scale vector file of building footprints with the number of floors as useful attribute for the land-cover classification improvement.

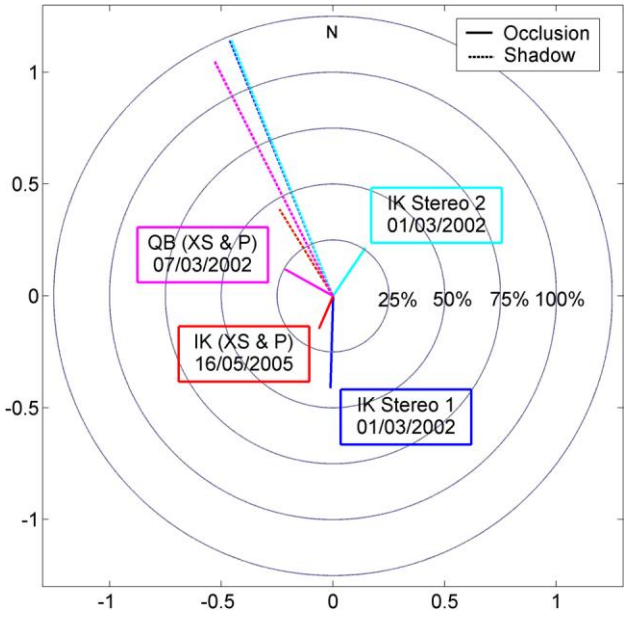

Figure 2: Shadow and occlusion directions on the three panchromatic Ikonos images used to produce the DSM and on the Quickbird image shown for comparison (shadow and occlusion lengths are given in % of the building height)

A nearly cloud-free time series of images at medium resolution consisting of 6 Landsat (E)TM images and a SPOT 5 image, spanning a period between 1987 and 2009, was acquired for the Istanbul study area.

Procedures and methods

The selected procedure is shown on the flowchart in figure 3. The area of 7 000 ha covered by the master Quickbird image was subdivided in three main zones: water, shadows and others. In each zone, a specific classification method was applied. Classification and post-classification of water bodies only used multispectral layers. Contrary to the classes “Shadow” and “Others”, for which classification and post-classification required the use of the building vector file and the DSM. Preparatory work, classification and post-classification are explained hereafter.

Preparatory work consists of three pre-processing, image fusion, image orthorectification and textural band computation.

The fusion of the multispectral and panchromatic bands of the master Quickbird image is based on a local statistics matching algorithm (vii). The fused images were used for visual interpretation during the classification and validation phases.

For the orthorectification of all the images, the same 25 Ground Control Points and the DSM extracted from the triplet of Ikonos images were used. Further developments in the photogrammetric processing task allowed the production of a higher resolution DSM (0.5 m) using tri-stereoscopic approaches (vii), but unfortunately it was not used at this stage of our research. The multispectral ortho-images were resampled at 2.4 m resolution for classification purpose.

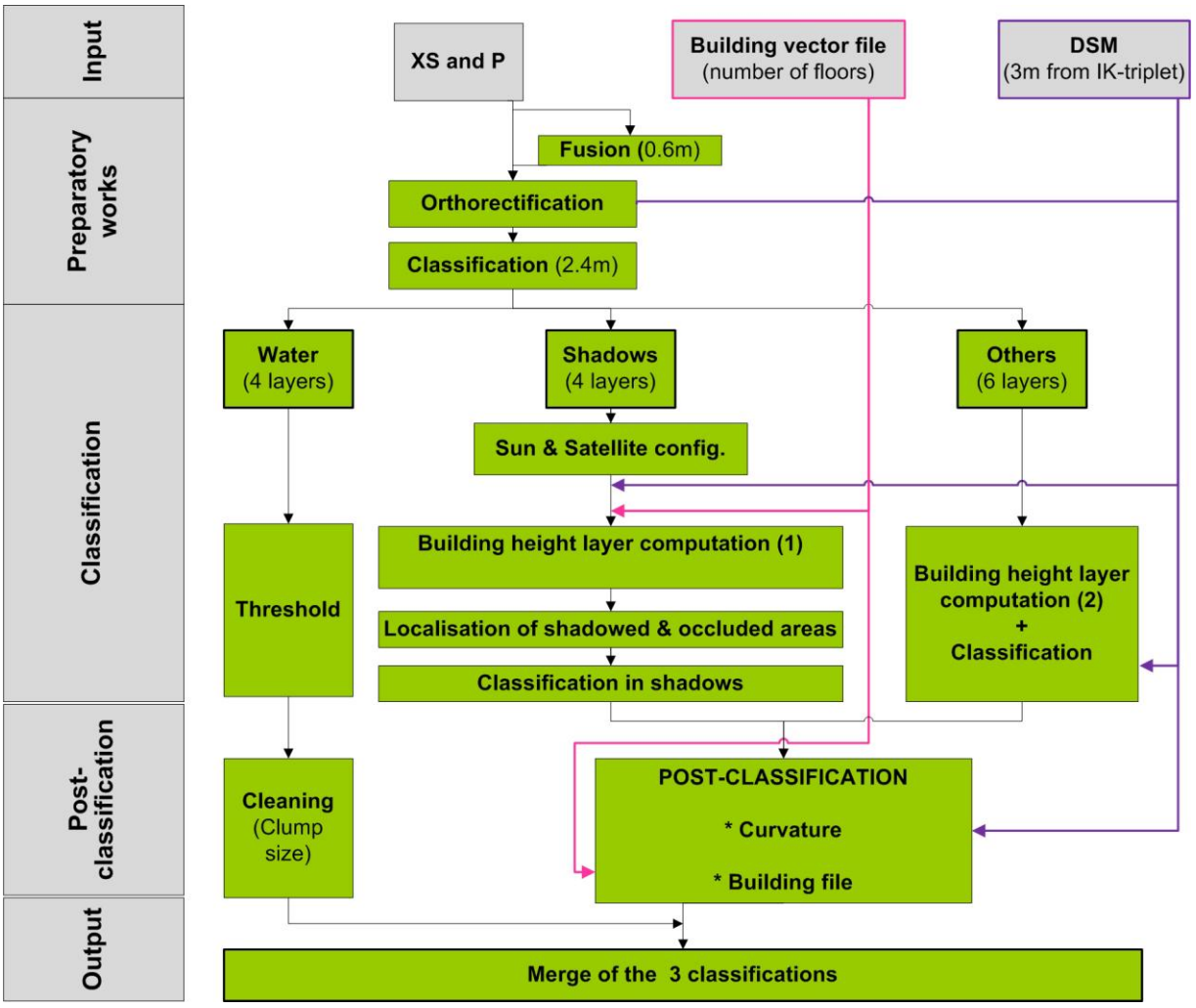

Figure 3: General workflow leading to the Istanbul classification.

An additional textural band was generated computing focal variance in a 7x7 window on the Quickbird panchromatic band, and was then resampled to the 2.4 m resolution. The decision to use the variance calculated on the PAN-band instead of other texture measures (e.g. Haralick co-occurrence measures) for improving the accuracy of the high-resolution (HR) classification was based on previous experience with HR image classification of urban areas in a former project (BELSPO-SPIDER). In this project it was shown that pixel-based land-cover classification of urban areas using different kinds of texture measures does not produce substantially different results in terms of classification accuracy even if the spatial pattern of the intensity values is taken into account by the coocurence and not by the variance. With respect to the choice of a 7x7 kernel size, we concluded from our previous work that in order to obtain improvements in urban areas with texture-based classification approaches, the window size should be smaller than or equal to the average size of the objects in the scene, which implies that for urban areas

the window size should be limited in extent. Our experiments showed that the variation of variance observed for different kernel sizes of limited extent is quite small.

Classification processes were independently applied on each of the three parts of the area (Fig. 3) using specific strategies. First, water bodies were obtained by thresholding NDVI, followed by a cleaning procedure based on clump detection, size analysis and mathematical morphology. Shadowed and occluded areas were determined next with the help of sun and satellite elevation and azimuthal angles (vii) provided in the image metadata (Table 1) and an improved DSM. Figure 4 illustrates the principle of the method applied to improve the DSM, producing more sharpened building shapes by using the building footprint vector file. This improvement aimed to better detect shadows by using the vector outlines of the large-scale building database. Furthermore, building height was calculated using a ground level altitude estimated at the building foot by a focal minimum extraction procedure and a flat roof altitude estimated by computing a zonal maximum in the footprint area.

Table 1: Metadata about sun and satellite positions of the master QuickBird image.

Angles	Azimuth			Elevation		
	Min	Max	Mean	Min	Max	Mean
(a) Shadows (solar)	153.2°	153.3°	153.2°	40.2°	40.4°	40.3°
(b) Occlusions (satellite)	109.4°	127.0°	119.0°	75.5°	76.8°	76.2°

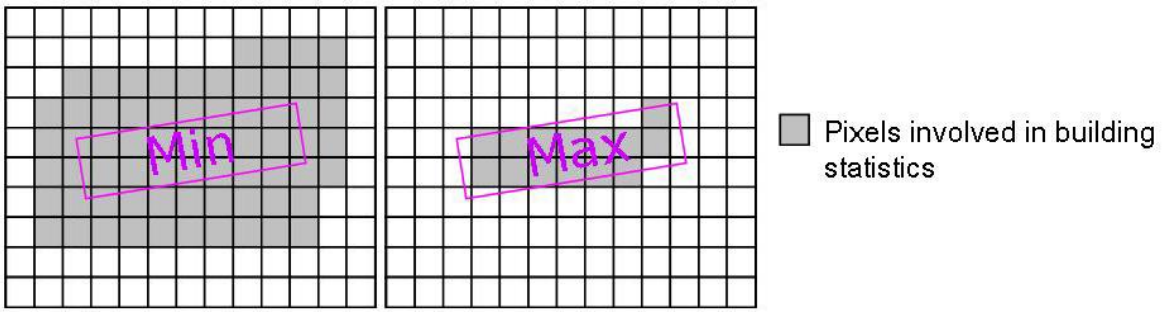

Figure 4: Reduction of the building bell-shape of the 3 m resolution DSM by replacing altitude around the building by a focal minimum 5x5 filter and by replacing altitude in the building footprint by the maximum observed in this footprint (flat roof)

The effect of this DSM improvement on shadow and occlusion detection is illustrated on figure 5. On Fig. 5_a, the shadow shown in dark grey spreads from the main building towards the north-west. The shadow area delineated from the original triplet DSM is shown in violet on Fig. 5_b. It covers a much smaller area than the actual one. Fig. 5_c shows the effect of the improvement procedure described above on the detected shadow. In a third version of the DSM, the attribute of the building database containing the number of floors was used to compute the building elevation using an estimated mean floor height of 2.62 m that was obtained from a sample of building heights estimated from shadow length. The height of all the buildings was then

computed using this mean value and the number of floors. It was added to the minimum in the area covered by the footprint. The shadowed areas were modelled again with this improved DSM. As stated on Fig. 5_d this approach produced the more accurate results.

Detection of occluded areas from the initial DSM produced poor results. An example of the detection of occluded areas obtained with the last improved version of the DSM can be seen in figure 4_e. As the image was not acquired in a nadiral position, building top displacements mask a portion of the image. One can notice that in the case of the Quickbird image acquired in 2002, these occluded areas are nearly completely overlain by shadows. Because of the redundancy of the 4 channels and the poor dynamic, classification in shadowed areas uses only the 4 multispectral channels to detect only 3 classes, building, road network and vegetation.

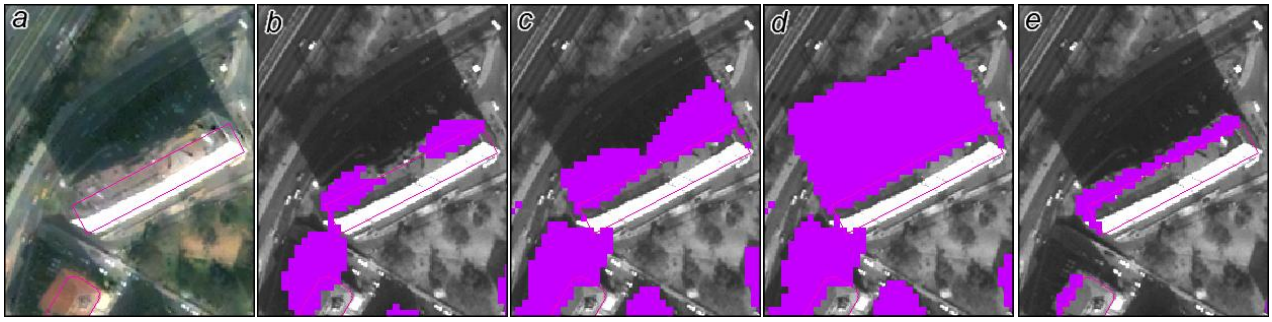

Figure 5: In violet shadowed and occluded areas detected with the initial DSM and after various DSM improvements

(a): Original image

(b): Shadows detected with the initial DSM

(c): Shadows detected with DSM improved by a focal minimum (5x5 kernel) to extract the ground level altitude around the building footprint and by considering a flat roof extracting the zonal maximum altitude from the DSM in the building footprint

(d): idem (c) but with a roof altitude as a function of the number of floors

(e): Occluded areas detected with the DSM used in (d)

Classification strategy adopted on the last spatial partition uses four Quickbird multispectral bands and the textural channel. Because it is obvious that urban classification can be improved by 3D information (vii), a neo-channel of building height derived from the initial DSM was also exploited. This last layer was determined by the difference between the initial DSM and a ground level surface obtained by an iterative procedure involving TIN creation from ground level points found by a sink detection procedure or focal minimum computation.

An unsupervised classification method was applied and its output was interpreted in homogenous and inhomogeneous classes. The latter classes were then submitted to a second unsupervised classification with a posterior interpretation. Finally, 26 sub-classes were obtained corresponding to 7 main classes (figure 9).

The post-classification procedures make use of the building vector file that presents updating lacks and/or incompleteness. As visible in the centre of figure 5, these lacks and incompleteness were revealed by DSM curvature computation using the partial second derivatives of a 2^{nd} order

polynomial function locally adjusted on the 9 altitude values of a 3 by 3 kernel. The result was then thresholded.

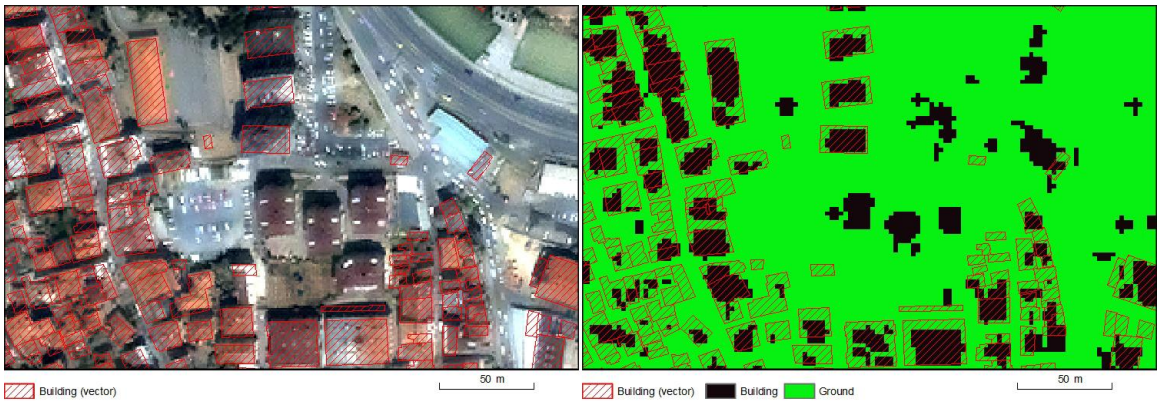

Figure 6: Updating lacks and/or incompleteness of the building vector file are partially revealed by thresholded surface curvature (see notably buildings in the image centre).

The final result of the classification procedure of the HR image is obtained by merging the 3 classified partitions.

RESULTS

Originally we intended to use an Ikonos image of 2005 as a substitute for the QuickBird image in shadowed and occluded areas. However, the 3-year time difference between the 2 satellite image acquisitions and the differences in vegetation phenology drastically reduced the possibility of doing so (Figure 7). So finally we decided to use only the QuickBird image.

Figure 7: Changes in vegetation cover are clearly visible in these 3 images, see e.g. the strip of vegetation dividing the parking space

(a) QuickBird (7th March 2002)

(b) Ikonos (16th May 2005)

(c) Recent aerial image (date of acquisition not available) taken from the Istanbul City Guide website http://sehirrehberi.ibb.gov.tr/map.aspx

Pixels classified as shadow (17%) and shadowed areas (83%) computed from the DSM represent more than 1 250 ha (19% of the emerged zone of the area covered by the image). Proportion in shadow and shadowed areas are: 89% for “Road network”, 6% for “Buildings” and

5% for “Vegetation”. Figure 8 gives an idea of the density of shadows in Istanbul’s Golden Horn. With the help of the DSM and the building vector file some pixels incorrectly assigned to the “road network” class were also moved to the “building” class.

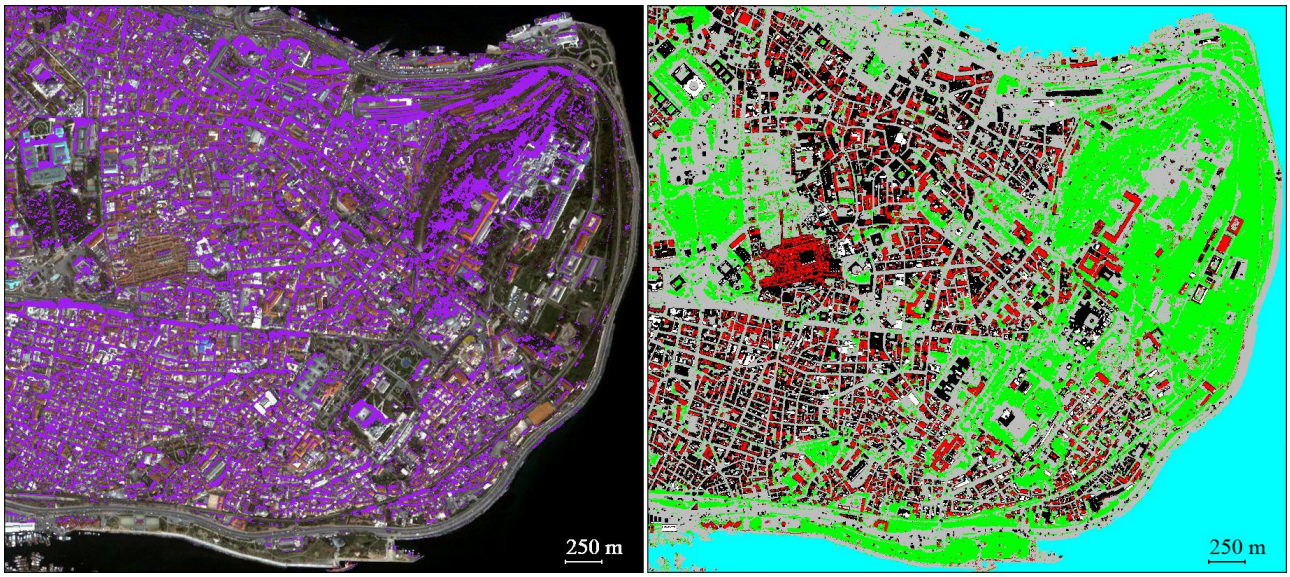

Figure 8: Shadow density (in violet) for the Golden Horn (left) and final classification of the same area (right) (legend is the same as on figure 8)

The final land-cover map produced consists of 7 classes (figure 9). To provide reference proportions of sealed surface cover and vegetation for training and validation of the sub-pixel classifier, classes were merged and spatially aggregated to the resolution of the Landsat or Spot imagery. A proper validation of the high-resolution classification is currently in progress.

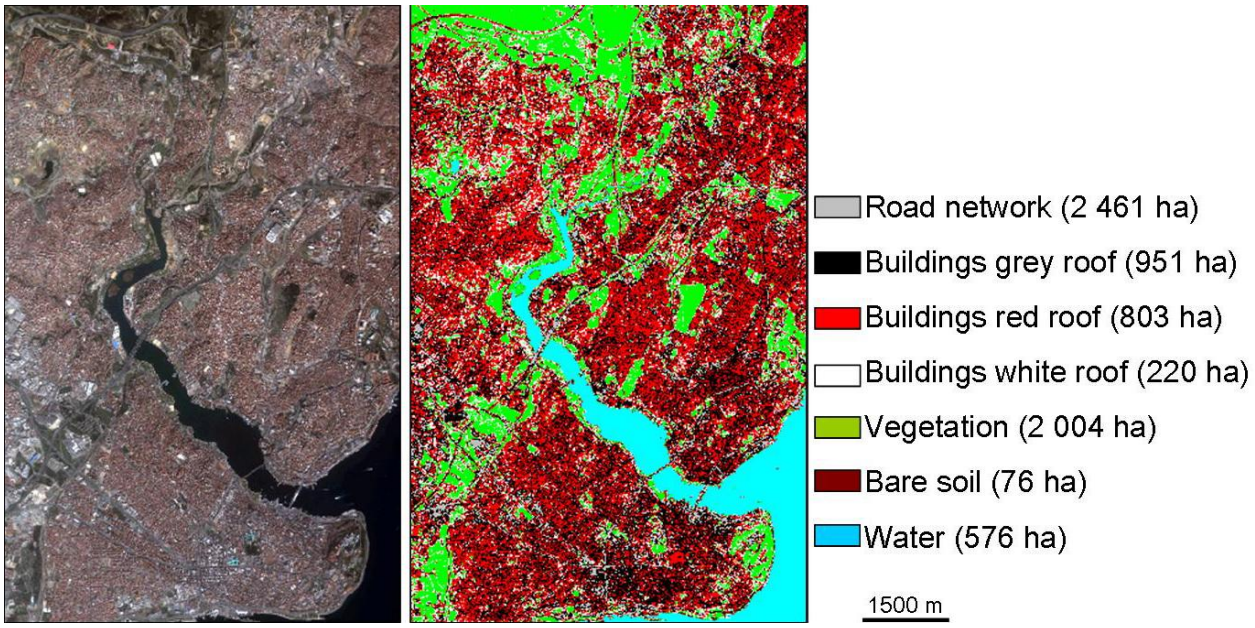

Figure 9: Final land-use/land-cover map of the Istanbul high-resolution study area (7 classes)

CONCLUSIONS

It can be concluded that the resolution of the triplet DSM (3m) remains relatively coarse for urban applications especially to solve problems in "urban canyons". An improved DSM at 0.5 m resolution was produced in the framework of the MAMUD project, but it has not yet been fully tested. Some trials show that very promising results can be expected.

Nevertheless major improvements can be noticed: (1) buildings not included in the vector file were detected by computation of curvature on the 3 m resolution DSM (2) this DSM also improved the detection of shadows and shadowed areas, and (3) we were able to distinguish three land cover classes in these shadowed areas.

Multi-image strategy to reduce problems of shadowed and occluded areas requires respectively the use of images acquired nearly synchronously with a complementary configuration and images taken in summer and/or taken at a another hour. These requirements will also be met by satellite constellations like PLEIADES. From this kind of satellite data we can also expect to produce more detailed DSMs. The improved version of the 3 m resolution DSM can be considered as similar to these DSMs or DSMs obtained from LIDAR data.

ACKNOWLEDGEMENTS

The research presented in this paper is funded by the Belgian Science Policy Office in the frame of the STEREO II programme – project SR/00/105. The authors also wish to thank Dr. G. Buyuksalih of IMP-Bimtas for making some Istanbul data available to us. More information about the MAMUD project can be found on http://www.mamud.be

REFERENCES

Rau J-Y, N-Y Chen and L-C Chen, 2002. True Orthophoto Generation of Built-Up Areas Using Multi-View Images. Photogrammetric Engineering & Remote Sensing, Vol. 68, N° 6, June 2002, 581-588.

Niehoffa D, U Fritscha & A Bronstert, 2002. Land-use impacts on storm-runoff generation: scenarios of land-use change and simulation of hydrological response in a meso-scale catchment in SW-Germany. *Journal of Hydrology*, Volume 267, Issues 1-2, 1 October 2002, 80-93.

Leuzinger S, R Vogt & C Körner, 2009. Tree surface temperature in an urban environment. *Agricultural and Forest Meteorology*, Volume 150, Issue 1, 15 January 2010, 56-62.

U.S. Environmental Protection Agency (USEPA). 2000. National Water Quality Inventory: 1998. Report to Congress. www.epa.gov/305b/98report.

Canters F, T Van de Voorde, O Batelaan, J Dams, YCornet, M Binard, G Goossens, D Devriendt, F Tack, G Engelen, C Lavalle & J Barredo, 2007. Measuring and Modeling Urban Dynamics: Impact on Quality of Life and Hydrology. Objectives and Methodology. In: Proceedings of the IEEE International Geoscience and Remote Sensing Symposium (IGARSS 2007), Barcelona, Spain, July 23-27, 2007, 1994-1997

Cornet Y, C Schenke, S De Bethune, M Binard & F Muller, 2003. Stratégies de fusion d'images P/XS basées sur les principes colorimétriques et l'Egalisation de Statistiques Locales. Bulletin de la Société Française de Photogrammétrie et Télédétection, 169, 35-45.

Tack F, R Goossens & G Büyüksalih G, 2009. Semi-automatic city model extraction from tri-stereoscopic VHR satellite imagery, The International Archives of Photogrammetry, Remote Sensing and the Spatial Information Sciences, Vol. 38, part 3 / W4, ISSN 1682-1750, pp. 89-96

Dare P, 2005. Shadow Analysis in High-Resolution Satellite Imagery of Urban Areas. Photogrammetric Engineering & Remote Sensing, Vol. 71, N° 2, February 2005, 169-177.

Zeng Y, j Zhang, G Wang & Z Lin, 2002. Urban land-use classification using integrated airborne laser scanning data and high resolution mutlti-spectral satellite imagery, in: Integrated Remote Sensing at the Global, Regional and Local Scale, ISPRS Commission I Mid-Term Symposium in conjunction with Pecora 15/Land Satellite Information IV Conference, 10-15 November 2002 (Denver, CO USA), ISSN 1682-1750